

## Manoeuvrability Prediction of Pure Car Carrier Installed with Schilling Rudder

K. Hasegawa, D.H. Kang, H. Nishikouri, H. Yamada\*, M. Yamaguchi\*\*, Y. Tanaka\*\* and T. Arii\*\*\*

Dept. of Naval Architecture & Ocean Engineering, Osaka University

Osaka, Japan

\*Tokimec. Co. Ltd

Tokyo, Japan

\*\*MOL

Tokyo, Japan

\*\*\*Japan Hamworthy Co. Ltd.

Osaka, Japan

### ABSTRACT

Manoeuvrability of pure car carrier (PCC) installed with Schilling rudder is discussed compared with the same ship installed with normal rudder. New type of PCC aiming to reduce wind resistance and to increase effective steering performance is investigated through the simulation and full-scale experiments. The hydrodynamic derivatives of the ship under consideration were predicted from those of the similar PCC already published. The numerical model of the ship was validated by comparison with full-scale trials. The wind resistance coefficients were predicted combining wind tunnel experiments and regression model. Numerical simulation was done for the performance under the constant wind and compared with some full-scale experiments. It is found the PCC with Schilling rudder is superior to the ship with normal rudder which was unable to control for certain relative wind direction.

**KEY WORDS:** PCC; Schilling rudder; wind resistance; manoeuvrability.

### INTRODUCTION

Recently many ships have been constructed with large superstructures especially in the case of PCC and LNG. The wind influence of those ships is more than that of conventional ships because of their large superstructures. Especially PCC is heavily affected by wind because the specific gravity of its cargo is very low.

In the actual voyage, wind resistance often causes ship's dislocation. The course keeping of PCC becomes very difficult when the wind resistance deviates its original course. In this case one should keep its original course using rudder control, and the resistance caused by rudder should be occurred. Further more the rudder deflection also causes the increase of ship's total resistance. Therefore the reduction and control of influence by wind are very important for the ship's performance in seaway.

Many researchers carried out the researches for the reduction of influence by wind such as Matsumoto(2003). In this research, the effective control device of maneuvering in wind is introduced. One way to improve manoeuvrability is to install shilling rudder. The shilling

rudder can provide larger rudder force compared with normal rudder. The paper shows the efficiency of the shilling rudder, which is confirmed by numerical simulation and the comparisons between the shilling rudder and the normal rudder.

### Model Ship

Two PCC's that have same hull forms are used for the numerical simulation. One is installed with normal rudder, and the other is installed with schilling rudder. The ships are downscaled the model ships whose LBP is 3m for the calculation. The scale ratio is 62.7. Particulars of the model ship are presented in Table 1.

Table 1. Principal particulars of model ship

$L_{BP}$	3.000m	$A_R / Ld$	0.019
$B$	0.514m	$\Lambda$	1.35
$d$	0.145m	$D_p$	0.105
$x_G$	-0.087m	$D_p / H_R$	0.992
$Cb$	0.539	$P / D_p$	1.042

### Equation of Motion

Surge, sway and yaw motion of a ship in winds are expressed by Eq. 1. Fig. 1 shows the coordinate system and definition of parameters.

$$\begin{aligned} m\dot{u}_G - mv_G r_G &= X \\ m\dot{v}_G + mu_G r_G &= Y \\ I_{ZZ}\dot{r}_G &= N - x_G Y \end{aligned} \quad (1)$$

where

$m$  : ship mass,

$I_{ZZ}$  : moment of inertia of ship,

$u_G, v_G, r_G$  : velocity and angular velocity at ship's center of gravity,

$x_G$  : distance between ship's center of gravity and ship's center.

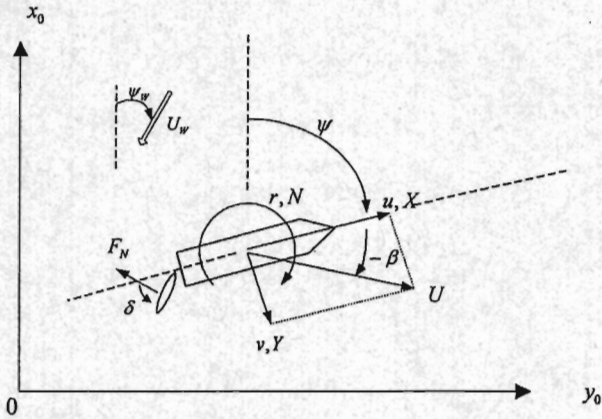


Fig. 1 Coordinate systems

The external forces  $X$ ,  $Y$  and moment  $N$  consist of hull, hull and propeller, rudder and wind components that noted with subscripts H, HP, P, R and A.

$$\begin{aligned} X &= X_H + X_P + X_R + X_A \\ Y &= Y_{HP} + Y_R + Y_A \\ N &= N_{HP} + N_R + N_A \end{aligned} \quad (2)$$

#### Hull Forces and Moment

Yoshimura(1986) proposed the equation and hydrodynamic coefficients for hull of the ship whose principal particulars are similar with the PCC that is adopted in this paper. Yoshimura's equations are used for estimating hull forces and moment, and the unknown hydrodynamic coefficients for hull forces also refer from those of Yoshimura's proposal.

#### Propeller Force

Mathematical model for thrust produced by propeller is expressed by Eqs. 3-4. Coefficients of thrust model from experiment data of objective ship are given in Table. 2.

$$X'_p = 2(1-t_p)K_T(D_p^2/Ld)/J_s^2 \quad (3)$$

$$\left. \begin{aligned} K_T &= a_1 + a_2J + a_3J^2 \\ J &= (1-w_{p0})u/nD_p \\ J_s &= U/nD_p \end{aligned} \right\} \quad (4)$$

Table 2. Coefficients of thrust model

$a_1$	0.566	$t_p$	0.165
$a_2$	-0.4593	$w_{p0}$	0.222
$a_3$	-0.0286		

#### Rudder Forces and Moment

Rudder forces and moment for normal rudder are assumed by Yoshimura(1986)'s proposal. Normal rudder and Schilling rudder that are used for calculations have the same size and aspect ratio.

**Schilling rudder.** The unique profile of the Schilling rudder incorporates a rounded leading edge and a fishtail trailing edge. The Schilling rudder is well known to control the propulsive force to achieve an efficient 'side thrust' effect at a ship's stern with operating angles up to 70 degrees. The figure and section of Schilling rudder are shown in Fig. 2.

Kido(1994)'s experiment is referred to estimate rudder forces and moment. Rudder normal force coefficient  $f_n$  of Schilling rudder for the calculations is assumed 1.3 times of one of normal rudder according to Kido's experiment.

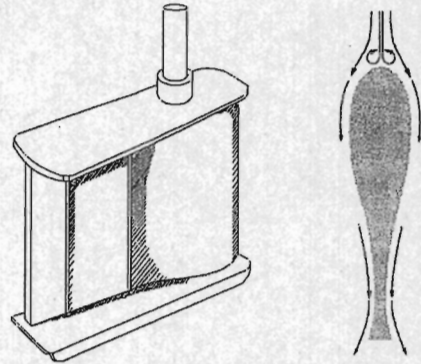


Fig. 2 Figure and section of Schilling rudder

#### Wind Forces and Moment

The steady forces induced by wind are considered. The expressions of the forces and moment induced by wind are as follow.

$$\left. \begin{aligned} X_A &= \frac{1}{2} \rho_A A U_A^2 C_{FX}(\Psi_A) \\ Y_A &= \frac{1}{2} \rho_A A U_A^2 C_{FY}(\Psi_A) \\ N_A &= \frac{1}{2} \rho_A A U_A^2 L C_{MZ}(\Psi_A) \end{aligned} \right\} \quad (5)$$

where

$\rho_A$  : mass density of air,  
 $A$  : effective projected area ( Breadth  $\times$  freeboard ),  
 $U_A$  : relative wind velocity,  
 $\Psi_A$  : relative angle of encounter wind,  
 $C_{FX}, C_{FY}, C_{MZ}$  : wind force coefficients.

The wind force coefficients of PCC that is used for simulation were found by wind tunnel experiment(Matsumoto, 2003). But only encounter angle from  $0^\circ$  to  $60^\circ$  had been tested at the experiment. Fujiwara(1994)'s estimation method are adopted to estimate wind force coefficients  $C_{FY}, C_{MZ}$  in the range that is not tested. In the case of  $C_{FX}$ , Wind resistance coefficient  $k$  that had been used at design stage are used to estimate coefficient  $C_{FX}$ . The coefficients that are estimated are fitted based on those from experiment. Wind resistance coefficient  $k$  is given in Fig. 3, and the parameters of Fujiwara are presented in Table. 3.

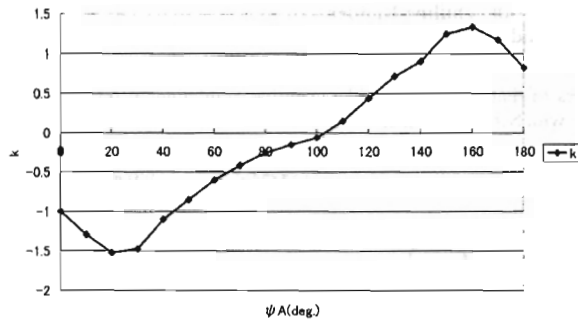


Fig. 3 Wind resistance coefficient  $k$

Table 3. Parameter of Fujiwara

$A_r$	0.261 m <sup>2</sup>
$A_L$	1.492 m <sup>2</sup>
$A_{OD}$	0.069 m <sup>2</sup>
$C$	-0.03 m
$C_{BR}$	-0.048 m
$H_{BR}$	0.363 m
$H_c$	0.156 m

#### Autopilot

Simple P-D controller is adopted for course keeping of the model ship. At the course keeping simulation, the order of rudder angle is simply controlled by Eq. 6. Coefficients are chosen as  $C_1=3.5$ ,  $C_2=0.9$  and  $C_3=50$  by the simulation.

$$\delta_{order} = C_1 \psi_e + C_2 r + C_3 d_e \quad (6)$$

where

$\psi_e$  : Angle of Deviation of heading angle from the original route,

$r$  : Angular velocity,

$d_e$  : Perpendicular distance between the ship and original route.

### CONSTRUCTION OF SIMULATION

Hydrodynamic derivatives of the PCC under consideration are unknown. For the simulation, it is necessary to estimate hydrodynamic derivatives.

#### Simulation with Normal Rudder

It is attempted to estimate hydrodynamic derivatives of objective ship referring from hydrodynamic derivatives of the PCC referred. The variation of hydrodynamic derivatives are assumed by the consideration of change of hull form, and the comparison between the simulation and the real ship's data of turning test and zig-zag test are performed with the varied hydrodynamic derivatives.

The sensitivities of hydrodynamic derivatives on 10° and 20° zig-zag test and 35° turning test are examined. The simulations with additional 20% of value of hydrodynamic derivatives are performed respectively. The index of sensitivity is the sum of squared value that is the difference of velocity between the simulation with the varied hydrodynamic derivatives and one without change. Only  $v$  and  $r$  is

considered, because initial velocity  $U_0$  is set at constant. After the change of hydrodynamic derivatives, the straight ahead running simulation is performed for finding the RPS of propeller to keep the initial velocity  $U_0$ . The sensitivities of hydrodynamic derivatives are calculated by Eq. 7, and Fig. 4 shows the results of the sensitivity examination.

$$S = \left( \sum_{t=0}^t (v_o(t) - v_s(t))^2 + \sum_{t=0}^t (r_o(t) - r_s(t))^2 \right) \times 100 \quad (7)$$

where

$S$  : sensitivity of hydrodynamic derivative,

$v_o, r_o$  :  $v, r$  in simulation without change of hydrodynamic derivative,

$v_s, r_s$  :  $v, r$  in simulation with change of hydrodynamic derivative.

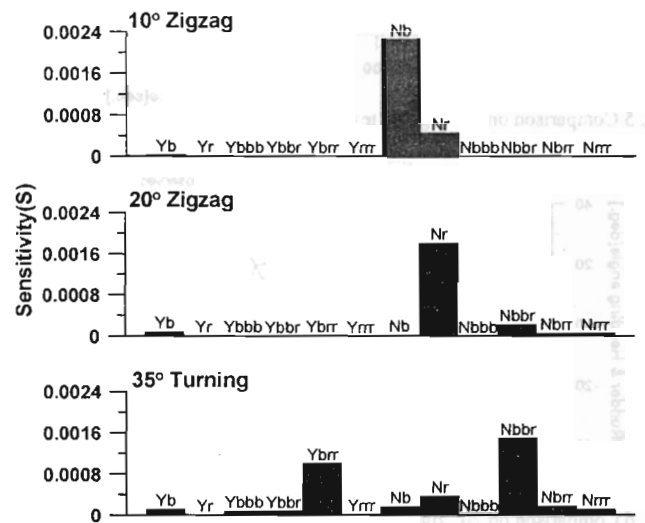


Fig. 4 Sensitivities of hydrodynamic derivatives

Table 4. Coefficients those are relative to the simulations

10° zig-zag test	$N'_\beta, N'_r$
20° zig-zag test	$N'_r, N'_{\beta\beta r}$
35° turning test	$Y'_\beta, Y'_{\beta r r}, N'_\beta, N'_r, N'_{\beta\beta r}, N'_{\beta r r}$

Hydrodynamic derivatives that are considerably relative to those tests are chosen, and shown in Table. 4. Try-and-error method is attempted to predict the value of hydrodynamic derivatives of PCC model. At first, the change of hydrodynamic derivatives for 10° zigzag test takes into the consideration, because 10° zigzag test has a few hydrodynamic derivatives that affect ship's sway and yaw, comparatively (Fig. 4). Only hydrodynamic derivatives that are chosen are changed, and the simulation is compared with the full-scale trials. The same method is performed for 20° zig-zag test and 35° turning test. The maximum variation of hydrodynamic derivative is set 30%, because the hull form of the ship under consideration is similar to the PCC referred. The variation of hydrodynamic derivatives from those of the PCC referred Yoshimura's ones are given in Table. 5.

Table 5. Variation of hydrodynamic derivatives from the PCC referred

$Y'_\beta$	20%	$N'_r$	30%
$Y'_{\beta rr}$	-25%	$N'_{\beta rr}$	25%
$N'_\beta$	-30%	$N'_{\beta rr}$	-20%

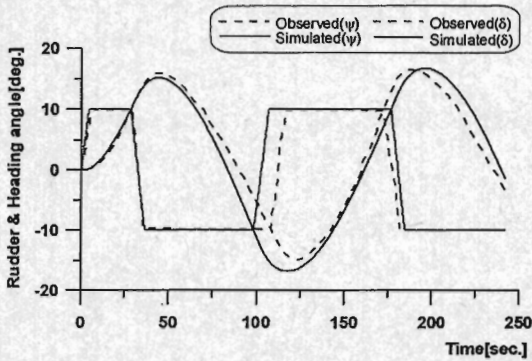


Fig. 5 Comparison on 10° zig-zag test ( $U_A=15.0$  m/s,  $\psi_A=15^\circ$  at start)

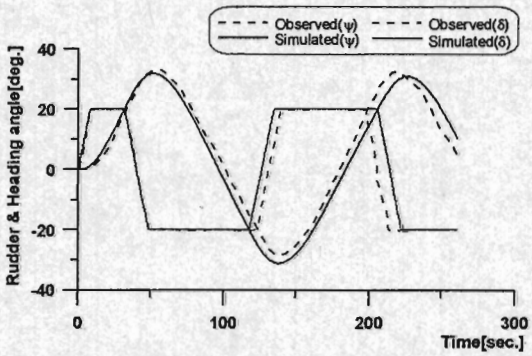


Fig. 6 Comparison on 20° zig-zag test ( $U_A=14.0$  m/s,  $\psi_A=10^\circ$  at start)

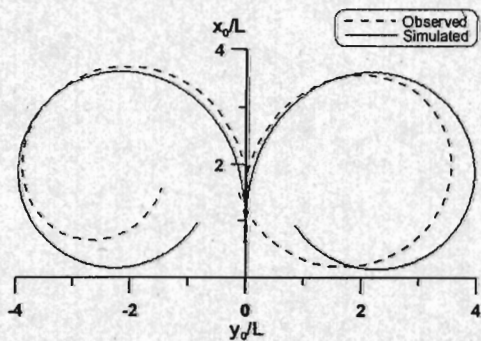


Fig. 7 Comparison on 35° turning test  
(Port:  $U_0=21.9$  knots, Starboard:  $U_0=20.8$  knots)

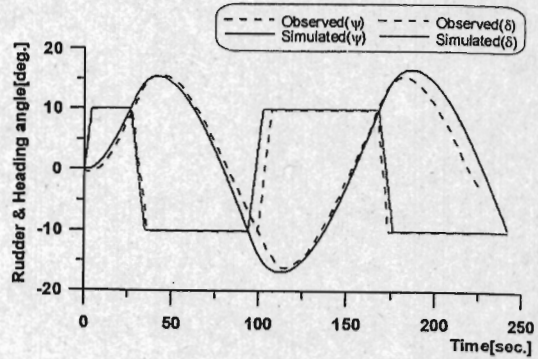


Fig. 8 Comparison on 10° zig-zag test with schilling rudder  
( $U_A=12.0$  m/s,  $\psi_A=10^\circ$  at start)

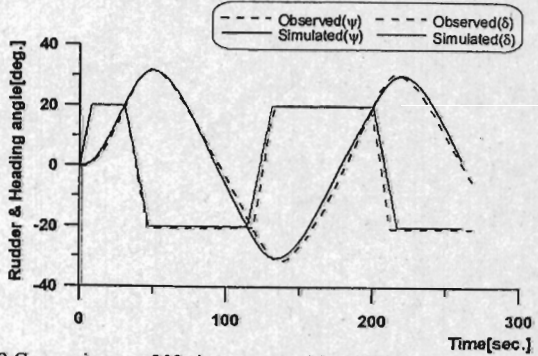


Fig. 9 Comparison on 20° zig-zag test with schilling rudder  
( $U_A=12.0$  m/s,  $\psi_A=10^\circ$  at start)

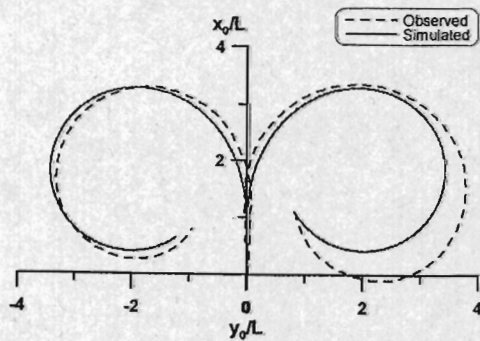


Fig. 10 Comparison on 35° turning test with schilling rudder  
(Port:  $U_0=19.8$  knots, Starboard:  $U_0=20.5$  knots)

The simulations with hydrodynamic derivatives those predicted are carried out. The comparisons between full-scale trials and the simulations of model ship are shown in Figs. 5-7. The simulations of 10° and 20° zigzag tests are in good agreement with full-scale trials, but the simulations of 35° turning test are of some disagreement, which might be caused by some disturbances in full-scale trials.

### Simulation with Schilling Rudder

Schilling rudder is incorporated into the same hull that is aforementioned. Nominal force coefficient of Schilling rudder  $f_a$  is set 1.3 times of that of normal rudder. Similar simulations were done for the ship with Schilling rudder.

Figs. 8-10 are the comparisons between simulations and full-scale trials. Even though Starboard 35° turning test in Fig. 8 shows the difference between two data, the adequacy of system which installed Schilling rudder is validated through the comparisons (Figs. 8-10). At the case of the Starboard 35° turning test, the reason of difference is

thought that full-scale trials has the influence of external forces such as wave and wind.

### SIMULATION IN WIND

The simulations of the ship installed with normal rudder and that installed with Schilling rudder are carried out to confirm the superiority of Schilling rudder. For this purpose, the simulation system in wind was established, and the simulation with Schilling rudder is compared with full scale trials to validate the system in wind. The comparisons of the simulation with both rudders are also done on course keeping in wind.

#### Simulation with Schilling Rudder in Course Keeping

The same simulation of real ship's data that are observed is performed to confirm the system. Full-scale trials were measured at Santander, Spain in 2003. The measuring trajectory is shown in Fig. 11, and the condition of observation is shown in table. 6.

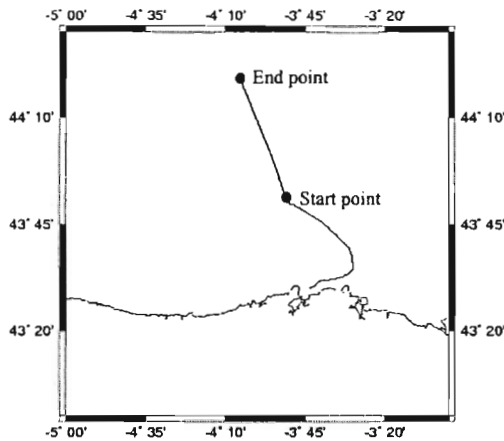


Fig. 11 Ship's trajectory at Santander, Spain

Table. 6 Observed data at Santander, Spain

Date of observation	2003.12.28
$U_{mean}$	6.95 m/s
$U_w$	19 m/s
$\psi_w$	-20 degree

Figs. 12~13 show the drift angle and the rudder angle of observed data in course keeping. The drift angle of real ship is calculated from Gyro and GPS data at an interval of 1 min. and the rudder angle is measured at an interval of 8 seconds.

The drift angle and the rudder angle of simulation in course keeping are shown in Figs. 14~15. There is the difference of rudder angle between the simulation and observed data in comparing mean value, because actual sea may give the effect of wave forces to the ship observed and the initial rudder angle due to torque of single propeller did not considered in the simulation. But the mean value of drift angle is similar with one of observed data.

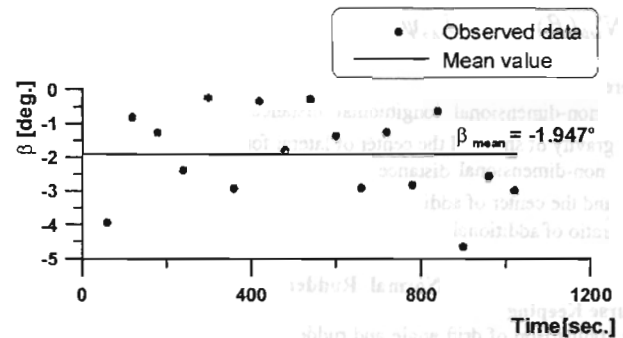


Fig. 12 Drift angle of observed data in course keeping

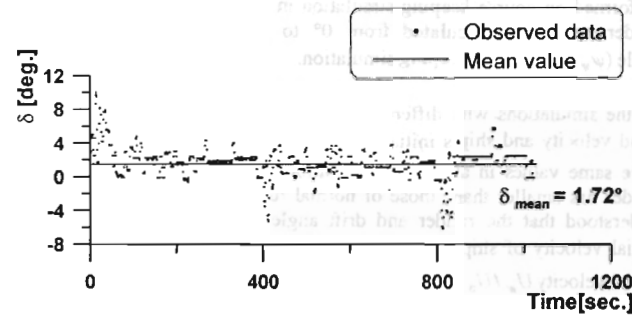


Fig. 13 Rudder angle of observed data in course keeping

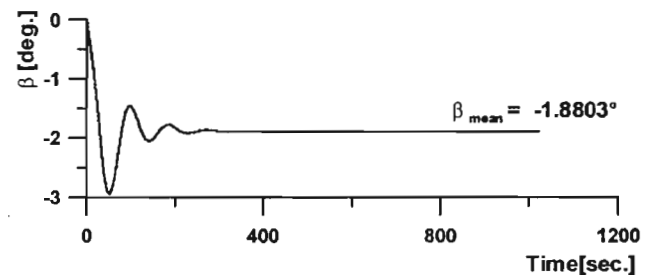


Fig. 14 Rudder angle of the simulation in course keeping

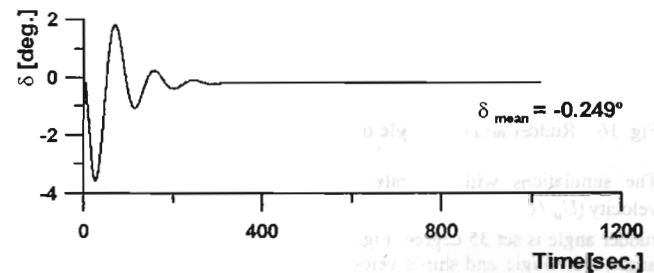


Fig. 15 Drift angle of the simulation in course keeping

Yasukawa(2004) shows the equilibrium equation (Eq. 8) of the relation between drift angle and wind. According to this equation, wind force and moment govern the drift angle of a ship. Therefore, the simulation system in wind is proper, and hydrodynamic derivatives for sway and yaw are also suitable, because the simulation and observed data have the similar value of drift angle under wind that is given.

$$\begin{aligned} & \{Y'_{HP}(\beta) + Y'_A(U_A, \psi_A)\}(x'_R + a_H x'_H) \\ & - \{N'_{HP}(\beta) + N'_A(U_A, \psi_A)\}(1 + a_H) = 0 \end{aligned} \quad (8)$$

where

- $x'_R$  : non-dimensional longitudinal distance between the center of gravity of ship and the center of lateral force,
- $x'_H$  : non-dimensional distance between the center of gravity of ship and the center of additional lateral force,
- $a_H$  : ratio of additional lateral force.

### Comparison between Normal Rudder and Schilling Rudder on Course Keeping

The comparison of drift angle and rudder angle between the ships, that are installed normal rudder and installed Schilling rudder, are performed on course keeping simulation in wind. The drift angle and rudder angle are calculated from  $0^\circ$  to  $180^\circ$  of encounter wind angle ( $\psi_w$ ) on course keeping simulation.

At the simulations with different initial velocity but the same rate of wind velocity and ship's initial velocity ( $U_w/U_0 = 4$ ), the drift angles have same values in all of the simulations but the angles of Schilling rudder has smaller than those of normal rudder (Fig. 16). It is easily understood that the rudder and drift angle are not governed by the initial velocity of ship  $U_0$  but by the rate of wind velocity and ship's initial velocity  $U_w/U_0$ .

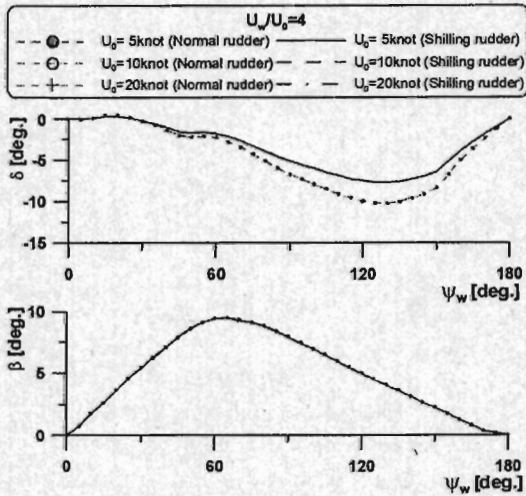


Fig. 16 Rudder and drift angle of the simulation in course keeping

The simulations with the rate of wind velocity and ship's initial velocity ( $U_w/U_0$ ) that are set 2, 4 and 6 are performed. The maximum rudder angle is set 35 degree. Fig. 17 shows the comparisons of rudder angle, drift angle and ship's velocity on course keeping simulation in wind. Both of drift angles and ship's velocities with normal rudder and Schilling rudder are equivalence at same wind condition in spite of the different rudder angles. But, out-of-control point ( $\diamond$ ,  $*$ ) appear at  $U_w/U_0 = 6$  simulation in the case with the normal rudder, but not in the case with Schilling rudder. Fig. 18 shows the time history of drift angle and rudder angle in simulation (out of control point  $\diamond$ ). In the simulation with normal rudder, rudder angle can not be set the certain angle to keep ship's route and oscillates, but the angle of Schilling

rudder is going to converge with the same control system. Fig. 19 shows the time history of lateral position and rudder angle in simulation (out of control point  $*$ ). In case of normal rudder, the ship can not keep her route with maximum rudder angle and ship's lateral position is diverged, but Schilling rudder is set the certain angle and keep ship's route at the same wind condition.

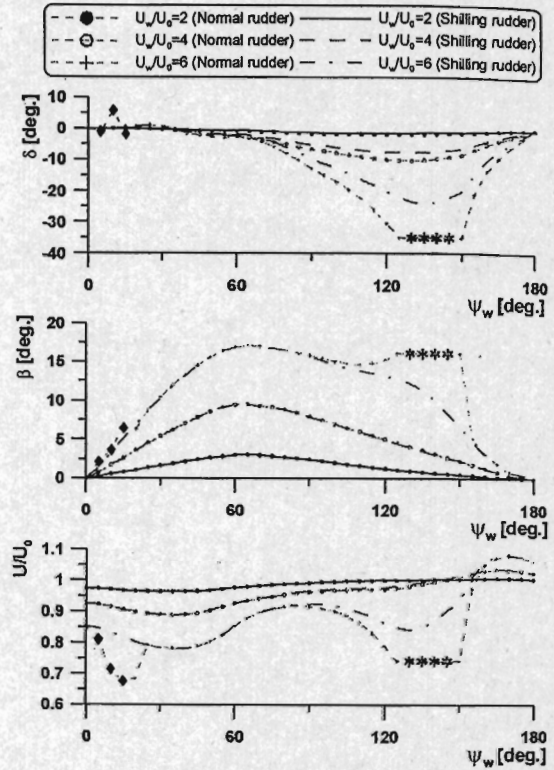


Fig. 17 Rudder angle, drift angle and ship's velocity in course keeping simulations

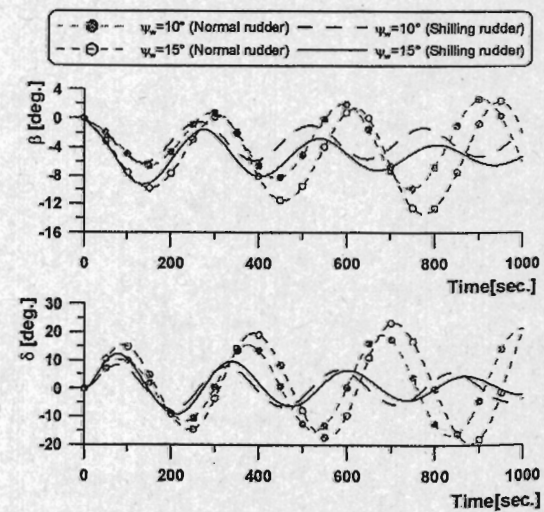


Fig. 18 Time history of drift angle and rudder angle in course keeping simulations

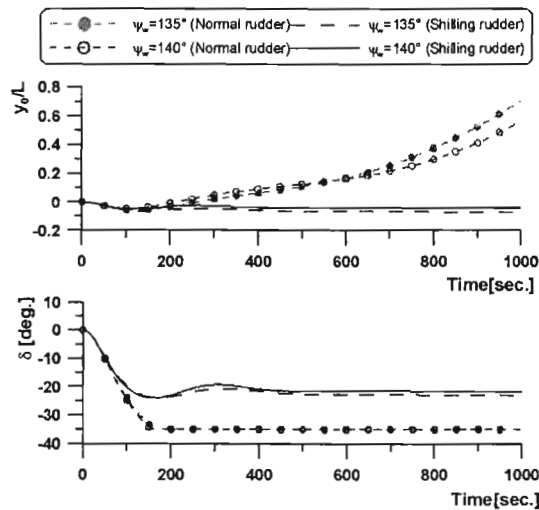


Fig. 19 Time history of lateral position and rudder angle in course keeping simulations

## CONCLUSIONS

In this paper, the way to improve maneuverability of PCC which is significantly affected by wind on sailing is discussed. Schilling rudder is one of the ways to improve its performance in wind. Therefore PCC with Schilling rudder is simulated, and the comparisons were done between normal rudder and Schilling rudder in case of course keeping in wind. Conclusions are drawn as follows.

1. Hydrodynamic derivatives of PCC that are unknown are predicted from those of the similar PCC and the ship's maneuvering is simulated successfully.
2. The rudder angle of Schilling rudder is smaller than that of normal rudder at same wind condition, even though the drift angle is same.
3. Normal rudder angle oscillates at the certain wind condition, but the angle of Schilling rudder converges to keep ship's route with the same control system.
4. Normal rudder with its maximum rudder angle can not keep ship's route at the certain wind condition, but Schilling rudder has the sufficient controllability at the same wind condition.

## REFERENCES

- Fujiwara, T., Ueno, M. and Nimura, T. (1998). "Estimation of Wind Forces and Moments acting on Ships," *J the society of naval architects of Japan*, Vol 183, pp 77-90. (In Japanese)
- Hirano, M., Takashina, J. and Moriya, S. (1984). "Ship Maneuverability in Wind," *J the society of naval architects of Japan*, Vol 155, pp 122-131. (In Japanese)
- Kido, T. (1994). "The feature of normal rudder and Schilling rudder," *Osaka Univ. Bachelor thesis*. (In Japanese)
- Matsumoto, K., Tanaka, Y., Hirota, K., Usami, S. and Takagishi, K. (2003). "Reduction of Wind Force acting on Ships," *J the kansai society of naval architects of Japan*, Vol 240, pp 115-121. (In Japanese)
- Rhee, K. P. and Kim, K. H. (1999). "A New Sea Trial Method for Estimating Hydrodynamic Derivates," *Ship & Ocean Technology*, Vol 3, No 3, pp 25-44.

- Yasukawa (2004). "Application of a Simulation Method for Ship Maneuverability to Maneuvering Booklet," *T the west-Japan society of naval architects*, Vol 107, pp 87-89. (In Japanese)
- Yoshimura, Y. (1986). "Mathematical Model for the Manoeuvring Ship Motion in Shallow Water," *J the kansai society of naval architects of Japan*, Vol 200, pp 41-51. (In Japanese)